DISTINCT ANATOMICAL CHARACTERISTICS IDENTIFY NOVEL MOLECULAR LAYER INTERNEURON SUBTYPE IN THE HIPPOCAMPAL DENTATE GYRUS

By

Fareed Rahman

A capstone project submitted for
Graduation with University Honors

May 31, 2020

University Honors
University of California, Riverside

APPROVED

_____
Dr. Viji Santhakumar
Department of Molecular, Cell, and Systems Biology

_____
Dr. Richard Cardullo, Howard H Hays Jr. Chair, University Honors

Abstract

Inhibitory interneurons in the dentate gyrus act as functional ‘gate’ or ‘filter’ by regulating cortical afferent input and enabling episodic memory processing. The dentate molecular layer contains the principal cell dendrites, which receive perforant path inputs. Diverse inhibitory neuron populations in the molecular layer, molecular layer interneurons (MLIs) are proposed to regulate the processing of these inputs. Although the dentate circuit has been widely studied, the structure and function of dentate molecular layer interneurons remain to be characterized.

MLIs were filled with biocytin in hippocampal slices during patch clamp recordings, imaged using confocal microscopy, and reconstructed using Neurolucida 360 for morphometric analysis. Based on the unsupervised cluster analysis of more than seventy somatodendritic parameters obtained from diverse MLIs, three distinct clusters were identified including previously described neurogliaform cells (NGFs), triangular cells (axo-axonic cells) and a novel class of cells, horizontal cells. Analysis of axonal spread revealed that horizontal cells have extensive molecular layer axon but also extend collaterals into the granule cell layer or hilus. Triangular cells had greater dendritic length and dendritic complexity than horizontal cells and NGFs. Functionally, both horizontal and triangular cells received significantly more frequent spontaneous inhibitory postsynaptic currents than NGFs. Horizontal cells may represent a novel class of dentate inhibitory neurons whose function needs to be analyzed further.

Table of Contents

Acknowledgements

First, I would like to thank the University Honors Program for providing me with the opportunity to engage in the three Honors Pillars of Excellence: Creating a Culture of Contribution, Promoting Creativity and Innovation, and Celebrating Diversity and Global Citizenship. My sincere gratitude goes out to all the staff, members, and faculty of the University Honors Program for their support and encouragement, without which this Capstone Project could not have been completed otherwise.

I would like to express my deep and sincere gratitude to my Faculty Mentor, Dr. Viji Santhakumar, MBBS, Ph.D., Associate Professor in the Department of Molecular, Cell and Systems Biology at the University of California, Riverside and Adjunct Associate Professor in Pharmacology, Physiology and Neuroscience at Rutgers New Jersey Medical School. Thank you for giving me the amazing opportunity to do research in your lab and for providing me with immeasurable support and guidance throughout the course of my undergraduate career. Your words of encouragement and sincerity have truly shown me the wonders of contributing to the scientific community and investing my time in the pursuit of knowledge.

I would like to give my wholehearted thanks to Dr. Akshay Gupta, MD for being my mentor in lab, teaching me a breadth of research techniques, and encouraging me to pursue excellence in research. I would also like to give many thanks to Andrea Esther Antony Therence Raj for being a wonderful and supportive research partner and for your continued hard work and dedication to the scientific community.

Lastly, I would like to express my utmost gratitude and gratefulness to my family. Thank you, from the bottom of my heart, to all in my family who have continued to support me throughout my undergraduate career.

List of Figures

Introduction and Background

The brain is a complex organ responsible for controlling all functions within the body, as well as interpreting and acting upon stimulus received from the external environment. While there are a number of different cells within the nervous system, neurons are nerve cells that serve as the primary building blocks and specialize in transmitting information. The path of transmission is dictated by the structure of neurons in which the key elements are dendrites, soma, and axons. Information is received through the dendrites and passed on to the soma, or cell body, which contains the nucleus of the cell. After passing through the soma, differences in membrane potential generate an action potential to transmit this information through axons. Axonal projections transmit activity/signals as all-or-none electrical events called action potentials. Axons extend to the target cell or tissue where they release chemical transmitters which in turn produce a response based on the electrical or chemical nature of the information.

Our study focused on using Wistar rat brains, a commonly used mammalian system to model human diseases, because of their behavioral, biological, and genetic similarities to humans. Within the brain, we focused on the hippocampus which is located deep within the temporal lobe and is the center for learning and memory. The hippocampus is involved in many aspects of health and disease, and it has been shown to be greatly affected in several psychiatric and neurological disorders such as hippocampal atrophy during early onset of Alzheimer's disease (Anand and Dhikav 2012). Diving deeper into the hippocampus, we directly studied a region called the dentate gyrus. The hippocampal dentate gyrus is the first processing station for sensory inputs coming from the entorhinal cortex to the hippocampus proper and serves as a filter for behaviorally relevant information (**FIGURE 1**).

Santiago Ramón y Cajal (1911)

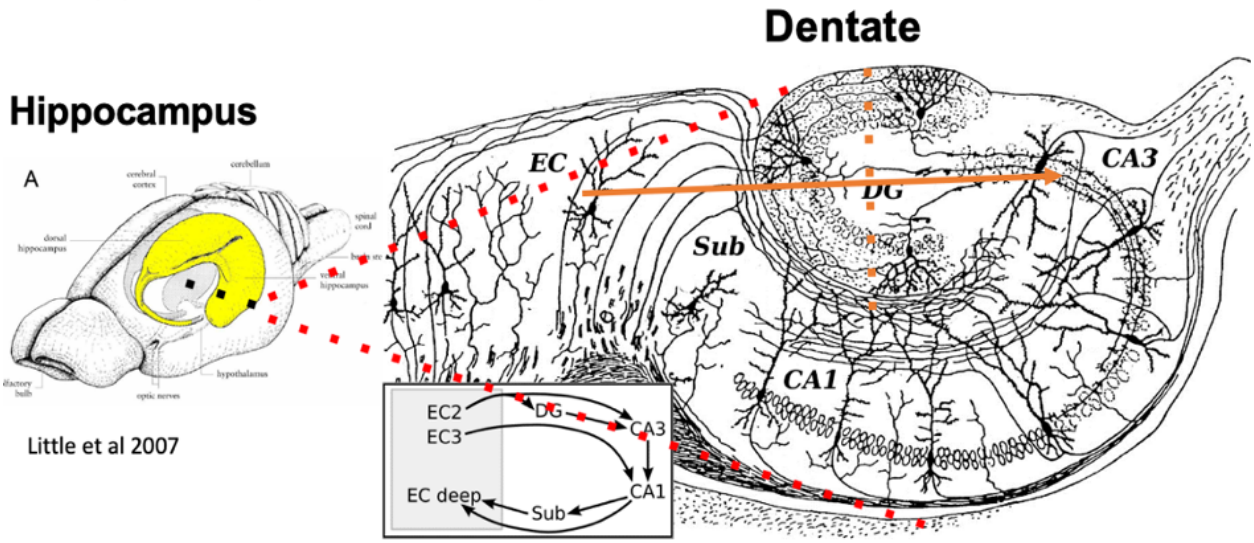

FIGURE 1: Hippocampal Dentate Gyrus – serves as the first processing station for sensory inputs coming from the entorhinal cortex to the hippocampus proper

The dentate itself consists of three layers: the hilus or polymorphic layer, which is the innermost layer, the granule cell layer which has the cell bodies of the projection neurons, and the outermost molecular layer (**FIGURE 2**). The molecular layer contains the dendrites of the principal cells from the granule cell layer, so it is the first layer to receive inputs from the entorhinal cortex through the perforant pathway.

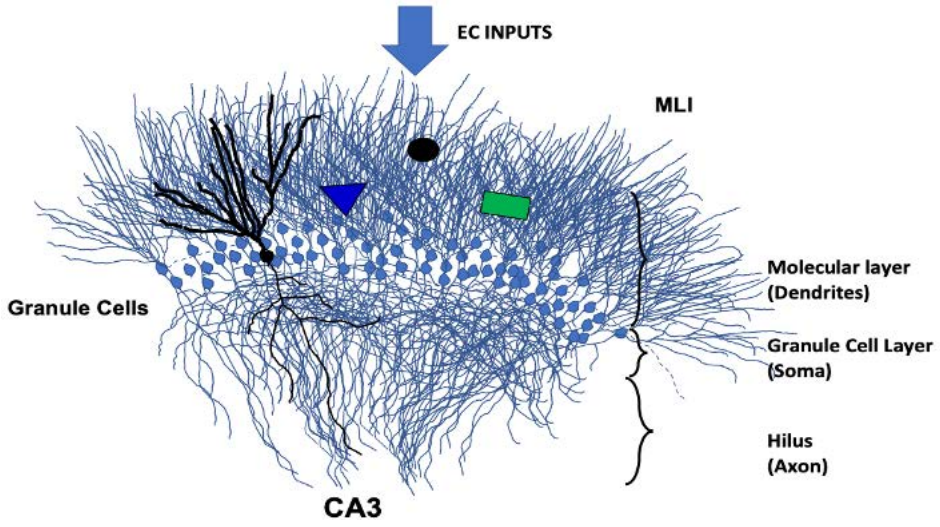

FIGURE 2: Three Layers of the Dentate Gyrus – molecular layer contains different interneuronal subtypes and is the first layer to receive entorhinal cortical inputs

Several inhibitory cell types have been characterized in the hippocampus and other cortical circuits (Klausberger and Somogyi Review 2008). In the dentate itself, the hilus has different inhibitory neurons such as somatostatin-immunoreactive GABAergic interneurons (Freud and Buzsaki 1996). However, not much is generally known about the outermost molecular layer, let alone the different inhibitory local circuit interneurons present within this layer. It has been proposed that molecular layer interneurons (MLI) are a population of diverse inhibitory neurons that regulate the sensory inputs. The goal of this study was to analyze the anatomical characteristics of these interneurons and classify them into discrete subtypes based on shared anatomical features. Neuronal somato-dendritic and axonal parameters are useful in examining not only morphology but can also play a role in determining the functional aspects of individual neurons. Through this process, a novel interneuronal subtype was also identified through this study.

Materials and Methods

Patch-Clamp Electrophysiology

Our primary approach to obtaining electrophysiological recordings was through the patch-clamp technique. Wistar rats (male aged postnatal day 25-35) were anesthetized with isoflurane and then decapitated. The brain slices were prepared in ice-cold sucrose artificial cerebrospinal fluid (aCSF, in mM: 85 NaCl, 75 sucrose, 24 $NaHCO_3$, 25 glucose, 4 $MgCl_2$, 2.5 KCl, 1.25 NaH_2PO_4, and 0.5 CaCl) and dissected using a vibratome into thin 300 µm slices, a size chosen in order to maintain a balance of keeping network connectivity in the hippocampus and surrounding areas as well as allowing for proper immunohistological staining to visualize under a confocal microscope afterwards. Sagitally bisected slices were then incubated at 32°C for 30 min in a submerged holding chamber containing an equal volume of sucrose-aCSF and recording aCSF (in mM: 126 NaCl, 2.5 KCl, 2 $CaCl_2$, 2 $MgCl_2$, 1.25 NaH_2PO_4, 26 $NaHCO_3$, and 10 D-glucose), and then held at room temperature afterwards. Solutions were saturated with 95% O_2 and 5% CO_2, maintained at a pH of 7.4 for 1–6 h, and slices were transferred to a submerged recording chamber and perfused with oxygenated aCSF at 33°C (Gupta et al. 2019). We then patched the cells in order to investigate the electrical properties of the molecular layer interneurons under infrared differential interference contrast and filled them with biocytin by adjusting voltage recordings (Gupta et al. 2012) (**FIGURE 3**). Biocytin is a useful compound because of its intracellular solubility, and it diffuses into the axon and dendrites of the live cells during recordings and allows us to make out the morphological details of the cells in the recording electrode after processing the tissue. It was particularly useful in this study for the visualization and recovery of fine morphological features such as terminal end visualization of neuronal dendrites. Furthermore, it was incredibly useful in determining thin axonal structures

that are normally spread out across the neurons. During these recordings, neuronal physiological properties including fire patterns were recorded for further functional characterization not presented in this report. The hippocampal slices were then fixed with 4% paraformaldehyde and then moved to a 0.1 M solution of Phosphate-buffered Saline to be stored before immunostaining of the cells.

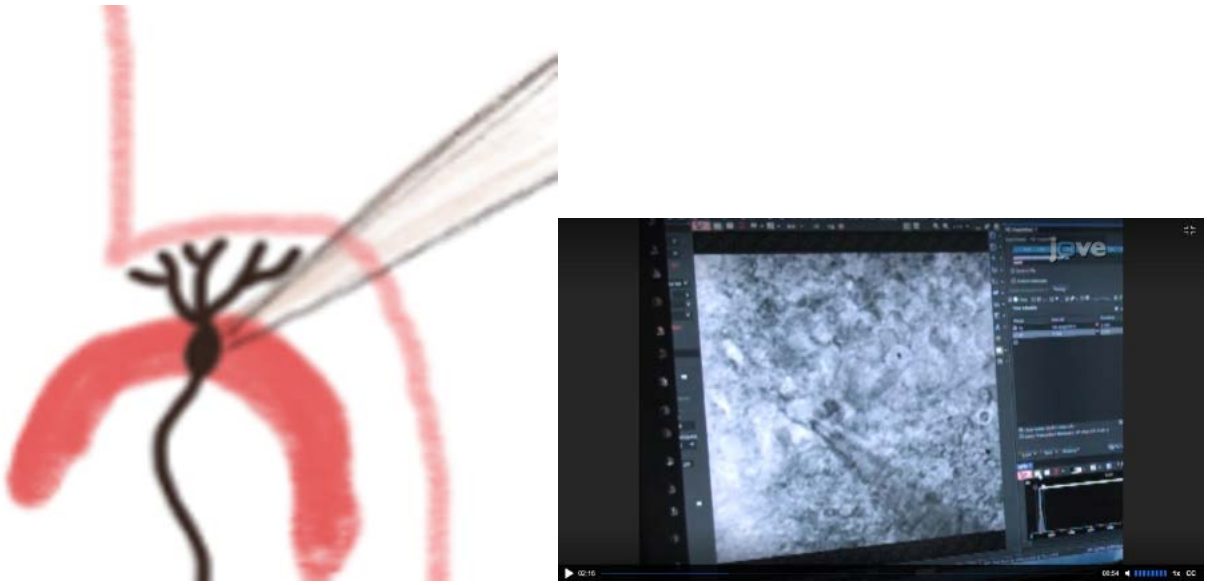

FIGURE 3: Example of Patch-Clamp Electrophysiology and Filling of Biocytin

Immunohistochemistry

After patching the cells in the molecular layer of the dentate gyrus and filling them with biocytin, we moved onto using techniques in immunohistochemistry to visualize the biocytin by reacting it with a fluorescent stain to enable its imaging using a confocal microscope. Immunohistochemistry is a procedure involving selective labeling of an antigen, in this case biocytin, by its association with a fluorescent dye. The brain slices were washed with 0.1 M Phosphate-buffered Saline, and the slices are then incubated in a streptavidin red dye conjugate, which selectively binds biotin in the biocytin. The biocytin staining was revealed using Alexa Fluor 594-conjugated streptavidin (Gupta et al. 2012). In order to protect the fluorescence and

potential re-staining, sections were mounted in an aqueous-based medium and coverslip edges were sealed with clear nail polish (Swietek et al. 2016).

Imaging

When imaging these cells, a Zeiss Inverted Confocal Microscope was used with water diffraction medium. In order to observe the fluorescence, lasers were used for excitation at 594 nm to observe factors such as the location, size, and extent of the molecular layer interneurons. Using the microscope, ideal imaging parameters were found to be 40X magnification, 1024 x 1024 frame size, and bidirectional scanning in the Z-plane. The frame size was kept at these dimensions in order to maximize efficiency of both the quality of the image and the length of time it takes to capture each cell image. Airyscan, a method of microscopy built into the system, was also used in order to generate high-resolution images with less constraint based on the size of the pinhole. When setting the Z-plane boundaries, careful consideration was taken to including the entire extent of both dendrites and axons in order to encompass the entirety of the cells. After locating the cell and establishing all parameters, images were obtained at a length of time relative to the size of the cell. The figure below presents a maximum intensity projection of a 3D stack that is generated through the bidirectional Z-plane imaging (**FIGURE 4**). The 3D nature of this imaging allows for the orientation of all neurons to be accounted for as their dendritic and axonal protrusions can extend in any direction.

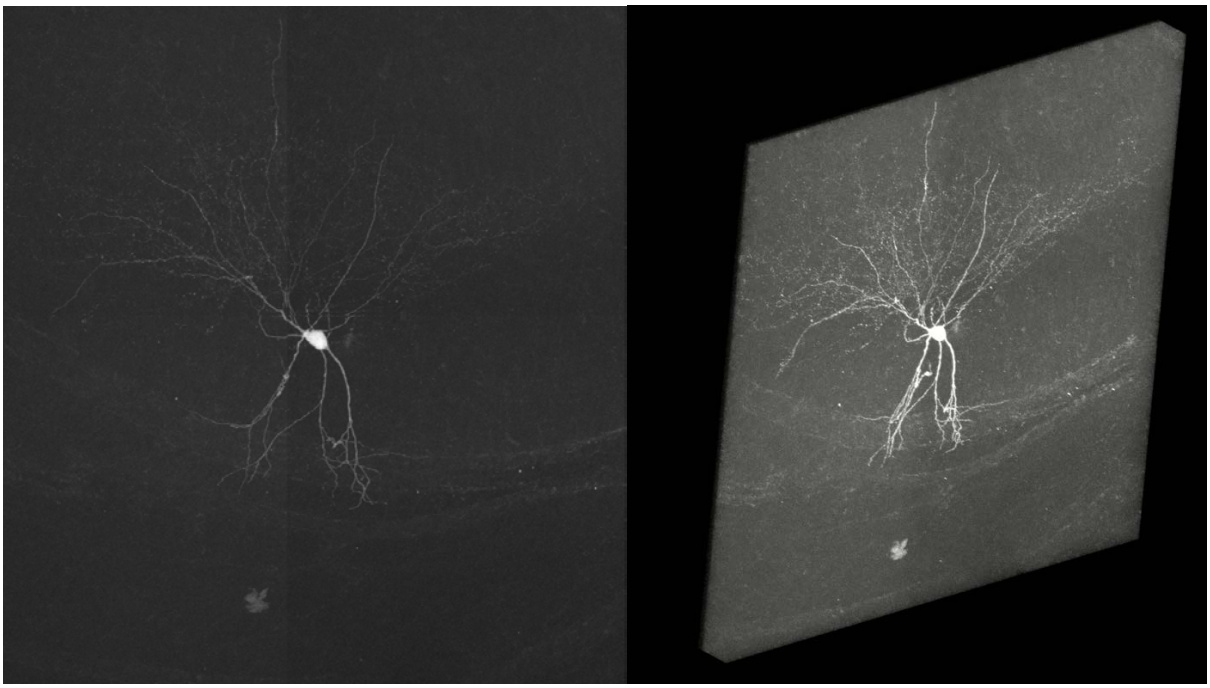

FIGURE 4: Fluorescence-based 3D Image under Zeiss Inverted Confocal Microscope – 100-micron Scale Included in Reconstructed Image on FIGURE 3

Neurolucida 360 / Neurolucida Explorer

After using techniques in patch-clamp electrophysiology, immunohistochemistry and confocal imaging, the last step before analysis of anatomical characteristics is producing three-dimensional models of the molecular layer interneurons. This was achieved using a specialized software platform known as Neurolucida 360 which allowed us to create user-guided 3D reconstructions of the various neurons (**FIGURE 5**). The program allows for the selection and specification of reconstructing different parts of the neuron such as the soma, axons, proximal dendrites, distal dendrites, and even axonal extensions from dendrites. A separate program, Neurolucida Explorer, is then used to generate measure quantitative morphological parameters from the reconstructions. These morphological data listed in Figure 13 and detailed in the Appendix (Tables 1 and 2) were used in the analysis of interneuronal subtypes. Many parameters

were used in analysis such as three-dimensional extent of axons, number of primary dendrites, node orders, and segment length among many others listed in FIGURE 13.

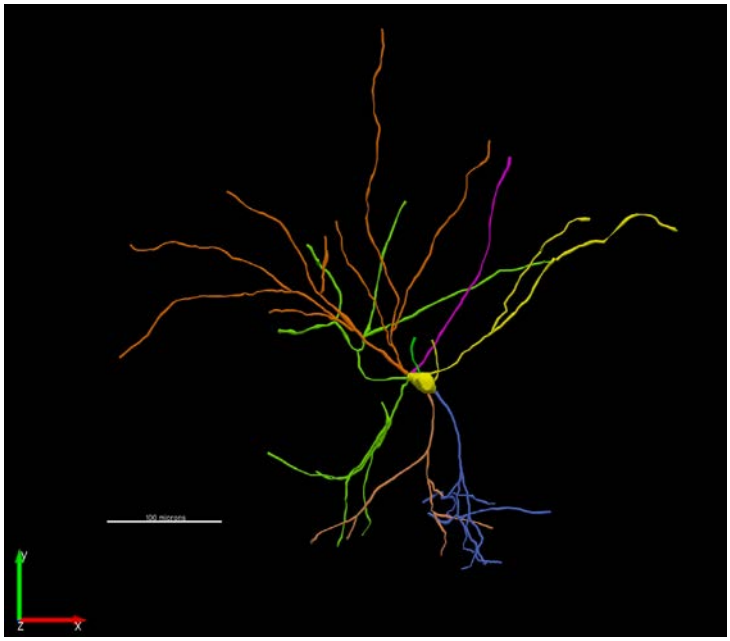

FIGURE 5: Neurolucida 360 3D Neuronal Reconstruction with 100-micron Scale Bar - 3D model above is the dendritic reconstruction of the cell shown in FIGURE 4

Unsupervised Cluster Analysis

Data were tested for uniform distribution and each quantified variable was fit to the sum of two or more Gaussian functions and quality of fit determined using maximum likelihood analysis (MLA; v2test) to assess normal distribution of parameters within each cell type. Variables with a nonuniform distribution were used for subsequent cluster analysis. A total of 71 somato-dendritic parameters from 35 morphologically reconstructed neurons, including both features measured in Neurolucida Explorer from the 3D reconstructions and parameters measured manually in 2D rendering (Neurolucida 360, MicroBrightfield) were analyzed. Unsupervised clustering and principal component analyses of morphological properties were conducted within R version 3.5.0, using R package Cluster, FactoMineR, and factoextra by an

investigator blinded to cell types and age groups. Hierarchical clustering on the selected principal components (PCs) was performed using Ward's Criterion with Euclidean distance to generate the dendrogram. The clustering partition was obtained from hierarchical clustering and improved with K-means method. Data are shown as mean±SEM (standard error of the mean). One Way ANOVA or Kruskal-Wallis One Way ANOVA on ranks was used to analyze data based on outcomes of Shapiro Wilk test for normalcy or equal variance test.

Results

Visual Differences

After careful reconstruction of thirty-five molecular layer neurons, it is noticeable that there is an obvious variety and visual difference between these cells (**FIGURES 6-11**). With scale bars of one-hundred microns included, there are cells on very opposite ends of the size spectrum. With anatomical differences, we began focusing on dendrites which are the structures that receive information before moving onto axons that distribute this information. There is a distinct difference in the way in which the dendrites are spread from the soma, or cell body, of the neurons. Further with dendritic analysis, we noticed that some cells have many more branches compared to others. These characteristics, among many others, were the basis for our visual categorization of molecular layer interneurons into distinct subtypes. Through Neurolucida Explorer, we generated reconstructions with dendrites color-coded based on branch order, which is determined when each dendritic branch splits into two or more branches (**FIGURE 12**). As seen between the two cells, green is the first branch order, red is the second branch order, purple is the third, and it continues in a similar fashion from proximal dendrites to distal dendrites based on the color-coding diagram illustrated in the legend.

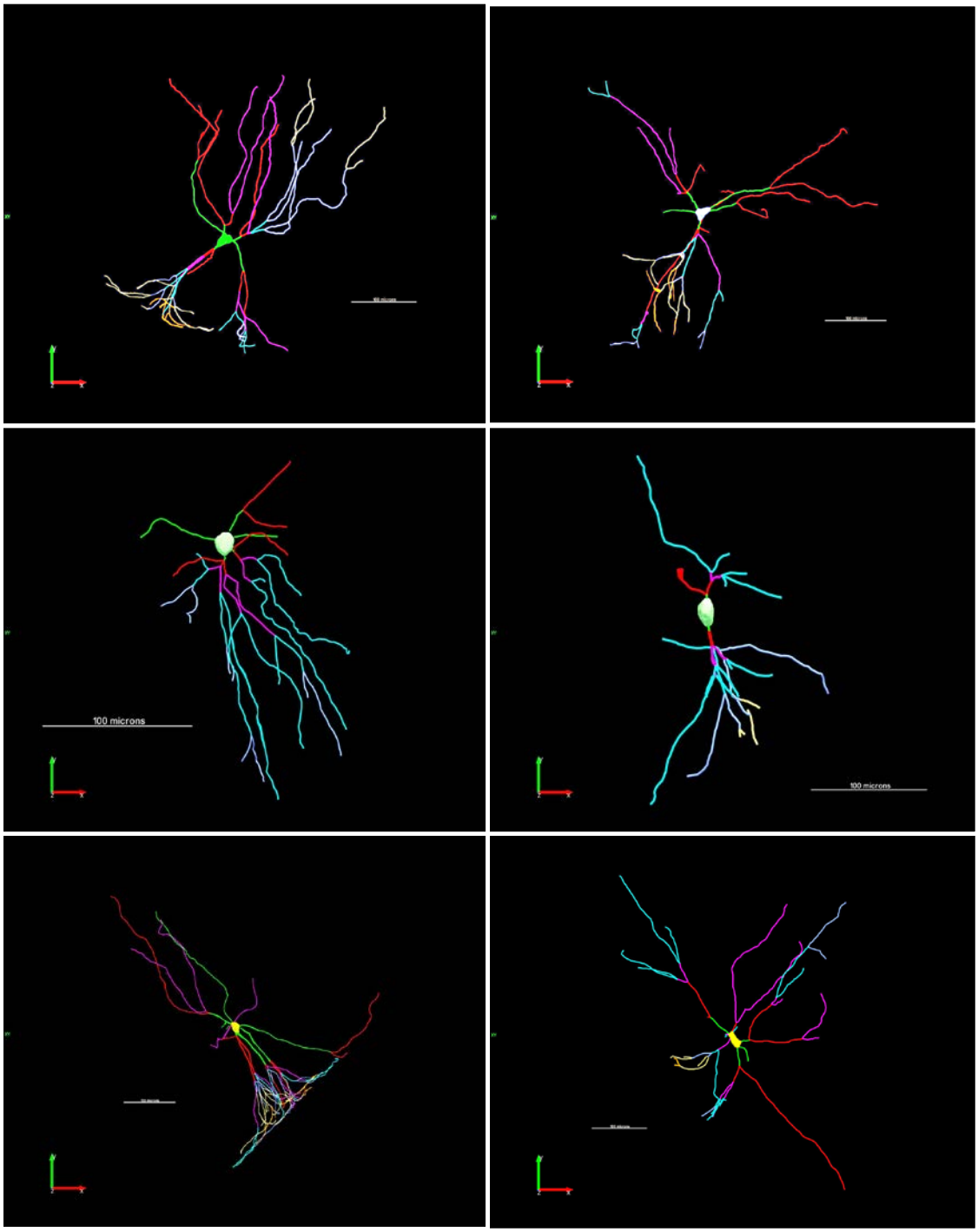

FIGURE 6: Reconstructions of Molecular Layer Interneurons (Cells 1-6) – 100-micron Scale Bar for Visual Comparison

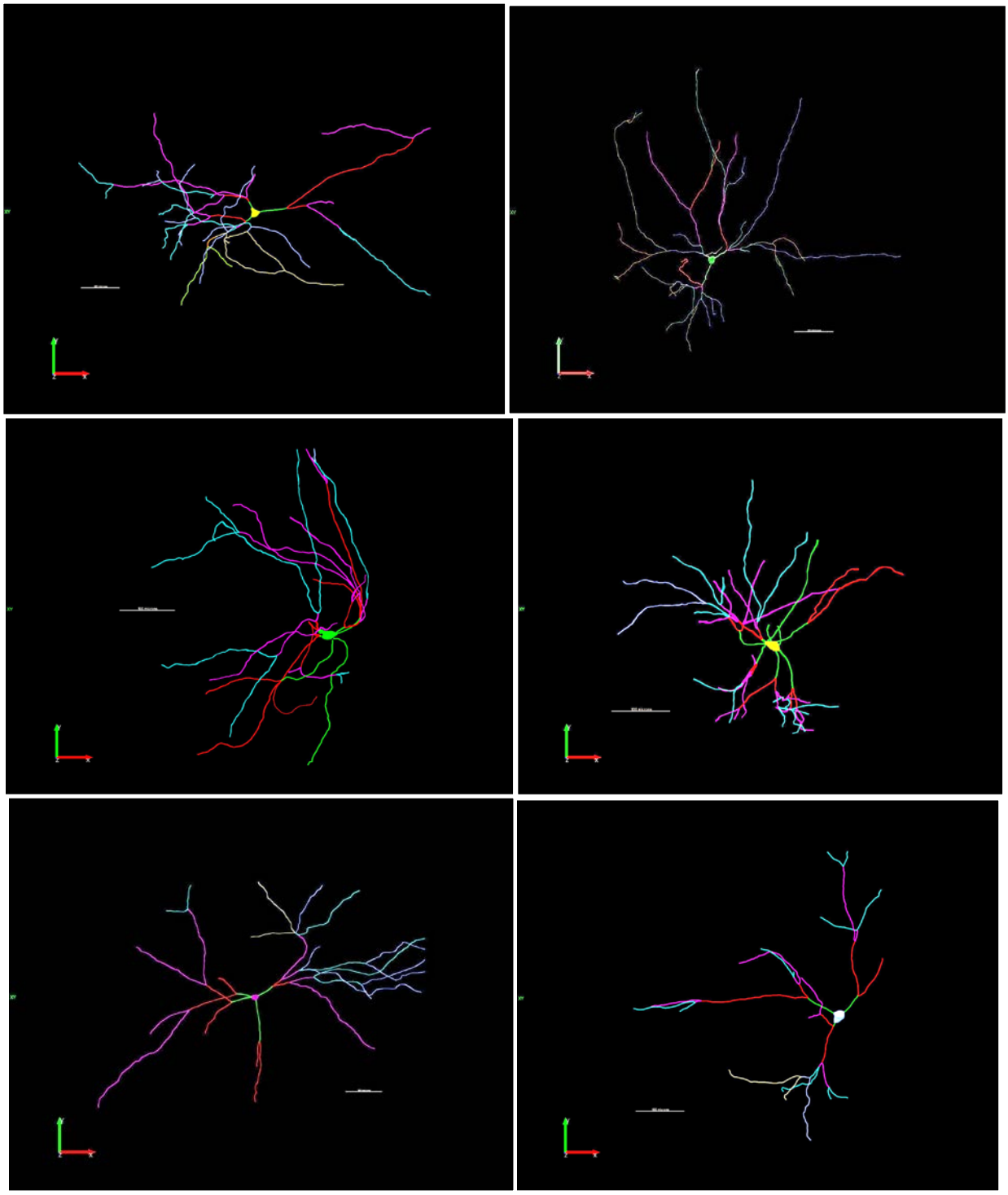

FIGURE 7: Reconstructions of Molecular Layer Interneurons (Cells 7-12) – 100-micron Scale Bar for Visual Comparison

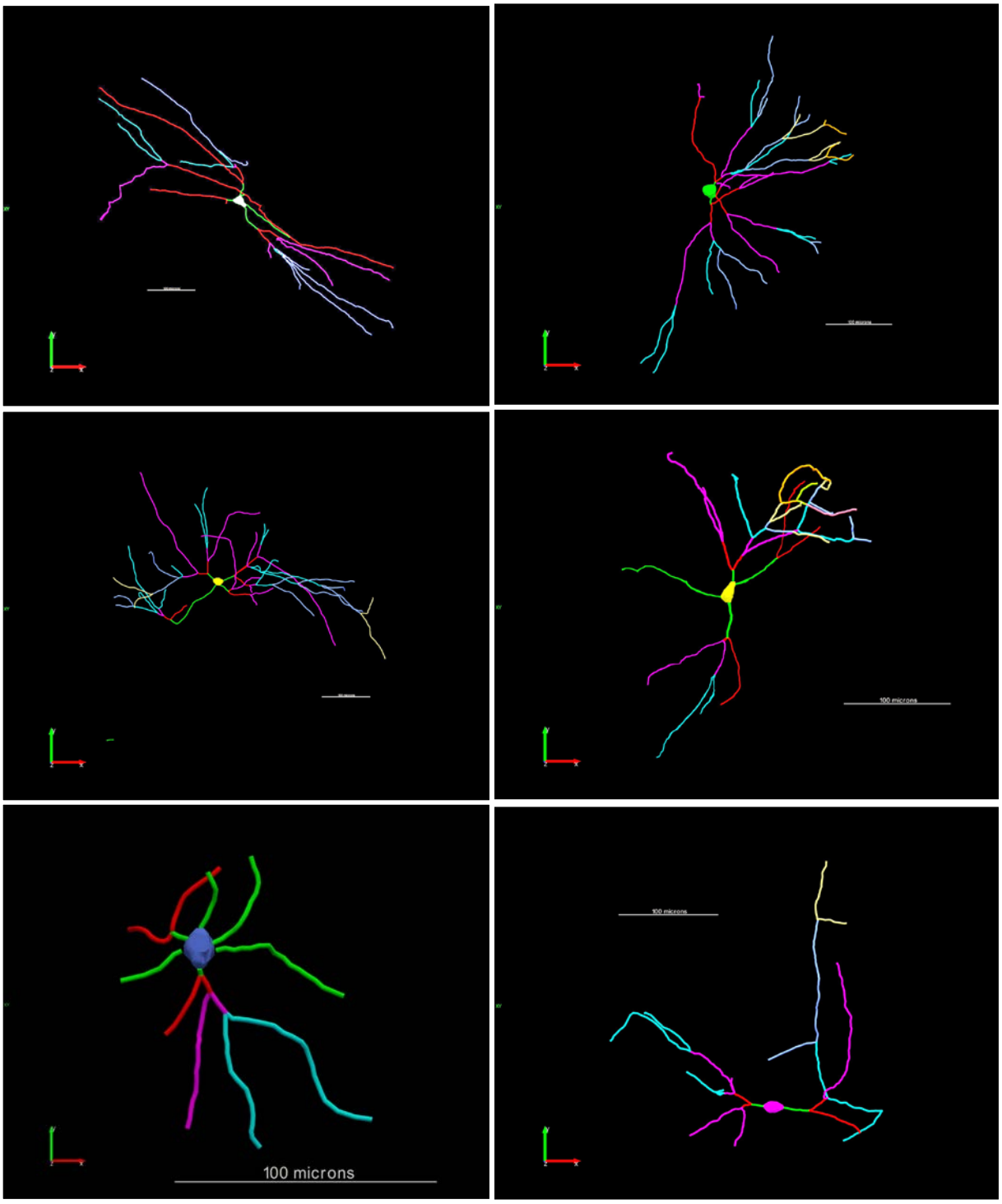

FIGURE 8: Reconstructions of Molecular Layer Interneurons (Cells 13-18) – 100-micron Scale Bar for Visual Comparison

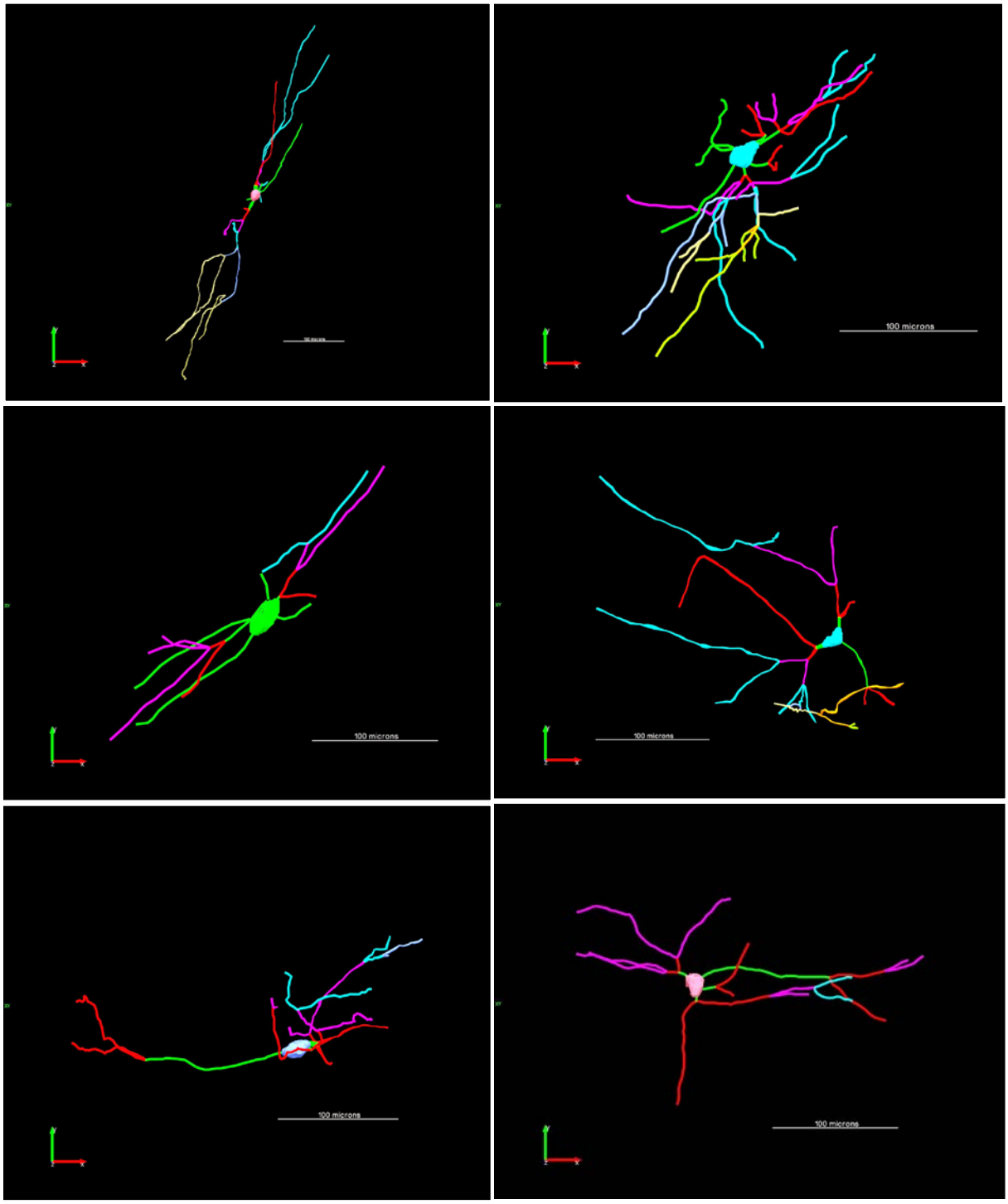

FIGURE 9: Reconstructions of Molecular Layer Interneurons (Cells 19-24) – 100-micron Scale Bar for Visual Comparison

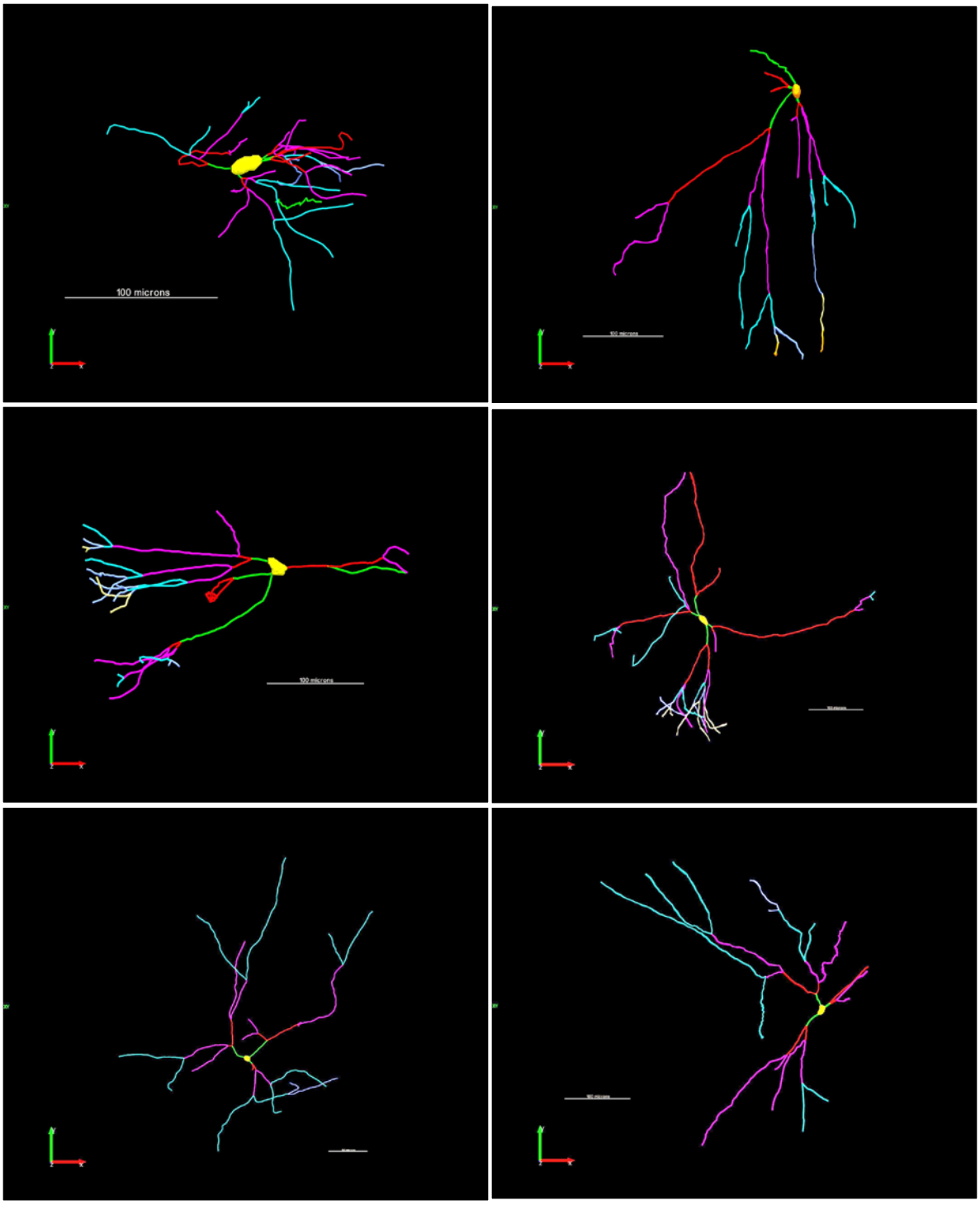

FIGURE 10: Reconstructions of Molecular Layer Interneurons (Cells 25-30) – 100-micron Scale Bar for Visual Comparison

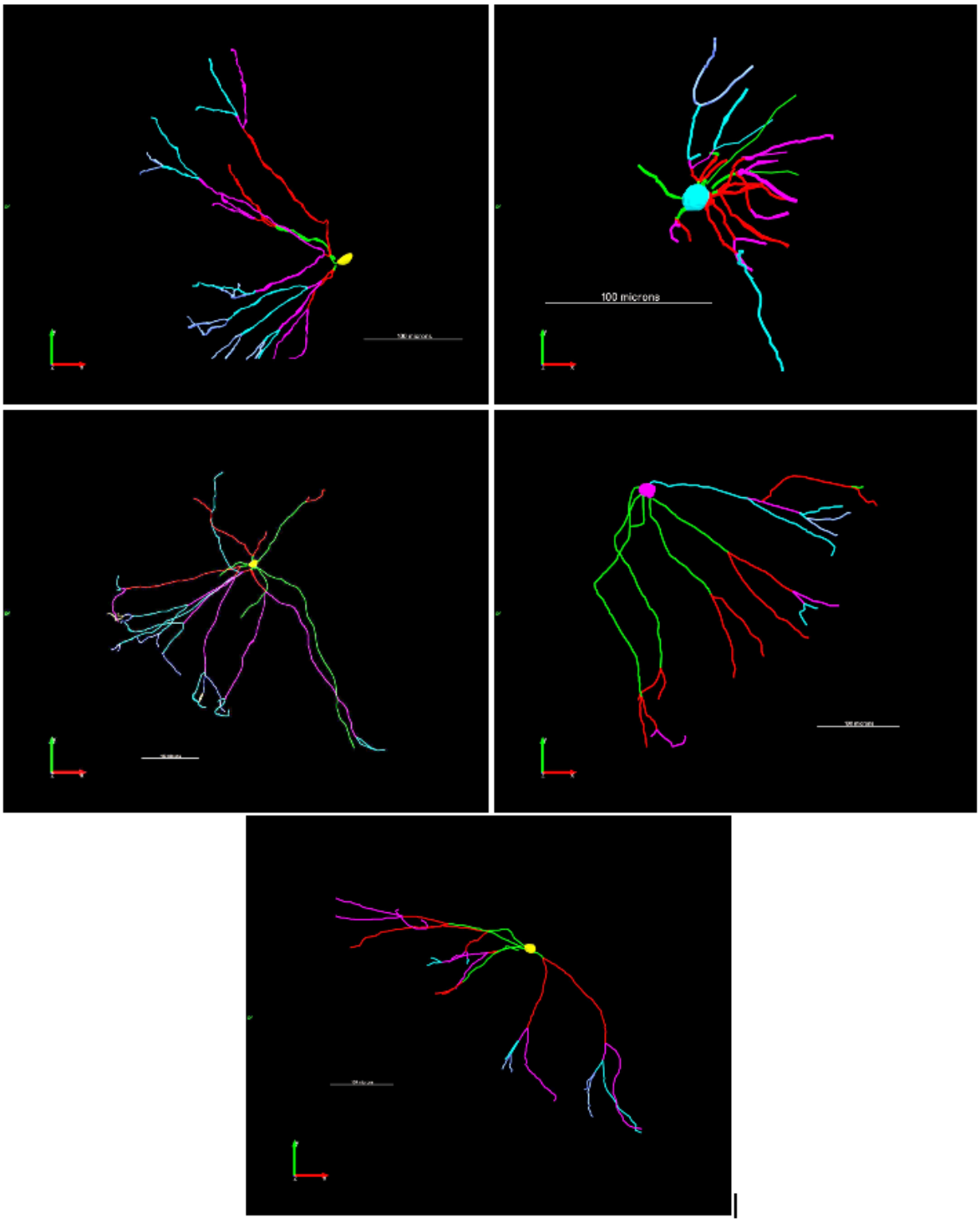

FIGURE 11: Reconstructions of Molecular Layer Interneurons (Cells 31-35) – 100-micron Scale Bar for Visual Comparison

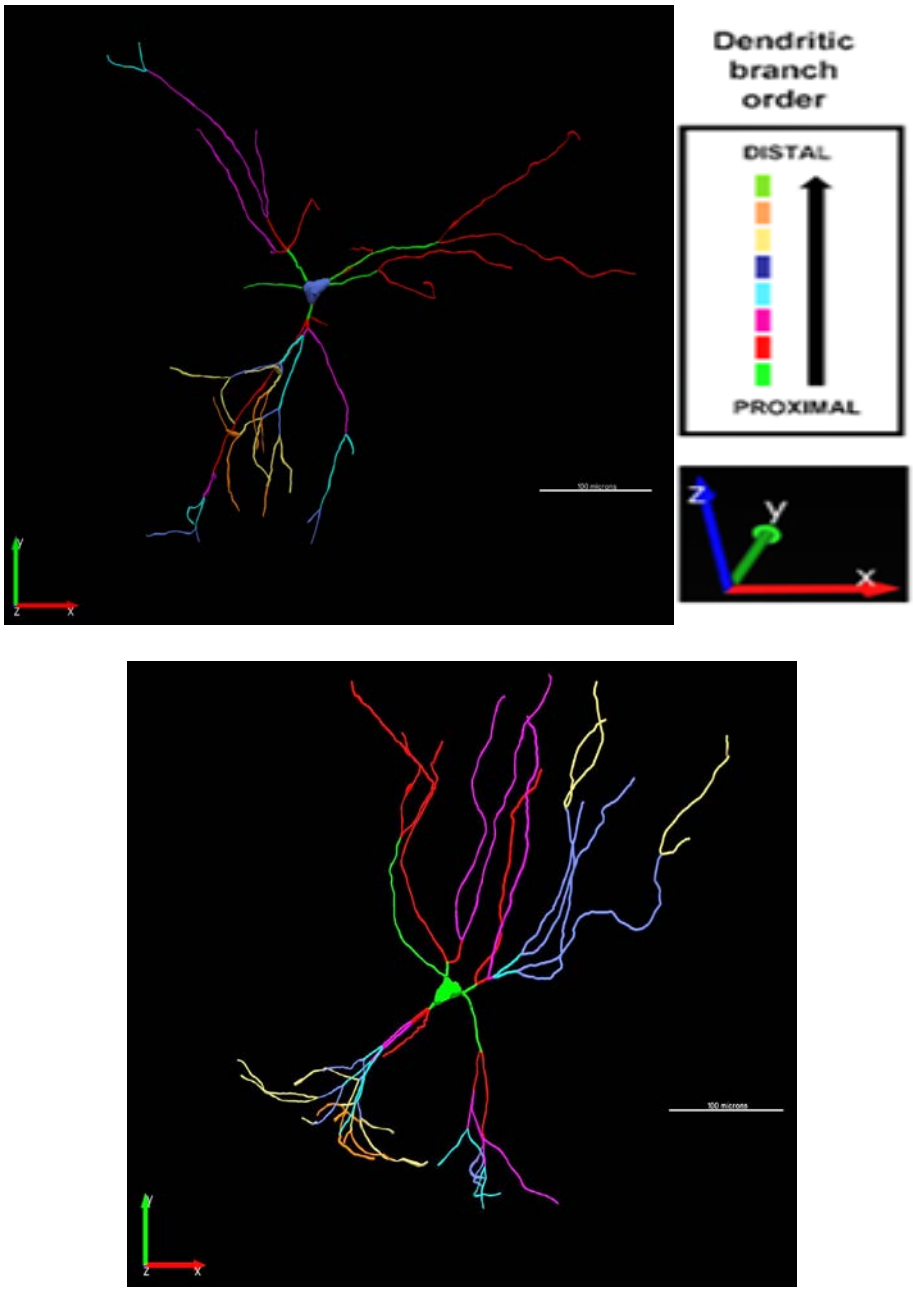

FIGURE 12: Branch Order Analysis and Branch Color-Code Diagram

Parameter Analysis

After noticing the immediate visual differences and observing the branch order, we were able to extract seventy-one objective parameters to further analyze the anatomical characteristics of these cells (**FIGURE 13**). These parameters are color-coded into categories for ease of differentiation between the different neuronal characteristics being analyzed: black for general

measurements and characteristics, blue for soma parameters, green for general dendritic parameters and node orders, purple for Sholl analysis of intersections, red for dendritic terminal ends, and yellow for the number and length of dendritic segments. Any mention of "order" within the parameters is based on branch order. For reference, nodes are the points at which one dendritic branch separates into two or more branches, intersections measure the variation between the number of branches and distance from the soma, and terminal ends refer to the distal ends of the dendrites. All objective parameters were selected and generated through excel sheets by using Neurolucida Explorer, and details of parameters are located in Appendix Tables 1-2.

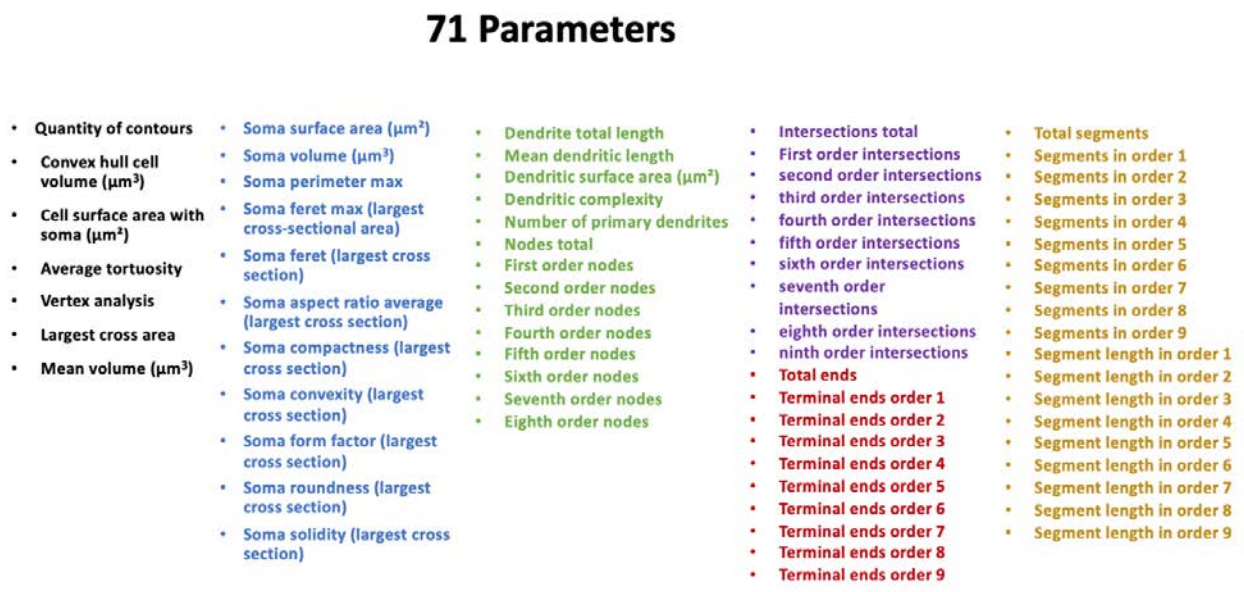

FIGURE 13: 71 Color-Coded Objective Parameters for Morphological Analysis of MLI

Hierarchical Cluster Analysis

After generating and compiling all sets of data with the seventy-one objective parameters for the thirty-five cells, we then presented our data to a statistician for principal component analysis. The purpose of this analysis technique is to increase the interpretability of large data sets without reducing the amount of information and maximizing the variance through new

uncorrelated variables. The statistician was blinded for the study in order to prevent bias when categorizing the cells into groups. After further analysis, she generated a dendrogram of a hierarchical cluster of the molecular layer interneurons (**FIGURE 14**). After uncovering the blinding and comparing the clusters with our previous estimations, we found that our cells had fallen into five categories as denoted by the colored boxes in FIGURE 14. The single cell in red was determined to be a projection neuron semilunar granule cell (SGC), a relatively new class on excitatory projection neuron and not an MLI. The reconstruction of the lone SGC included in the dataset is depicted for reference (**FIGURE 15**). The remaining four clusters were Neurogliaform cells, a novel class of horizontal cells, and two clusters with a triangular somata that included cells classified as axoaxonic or other triangular cells.

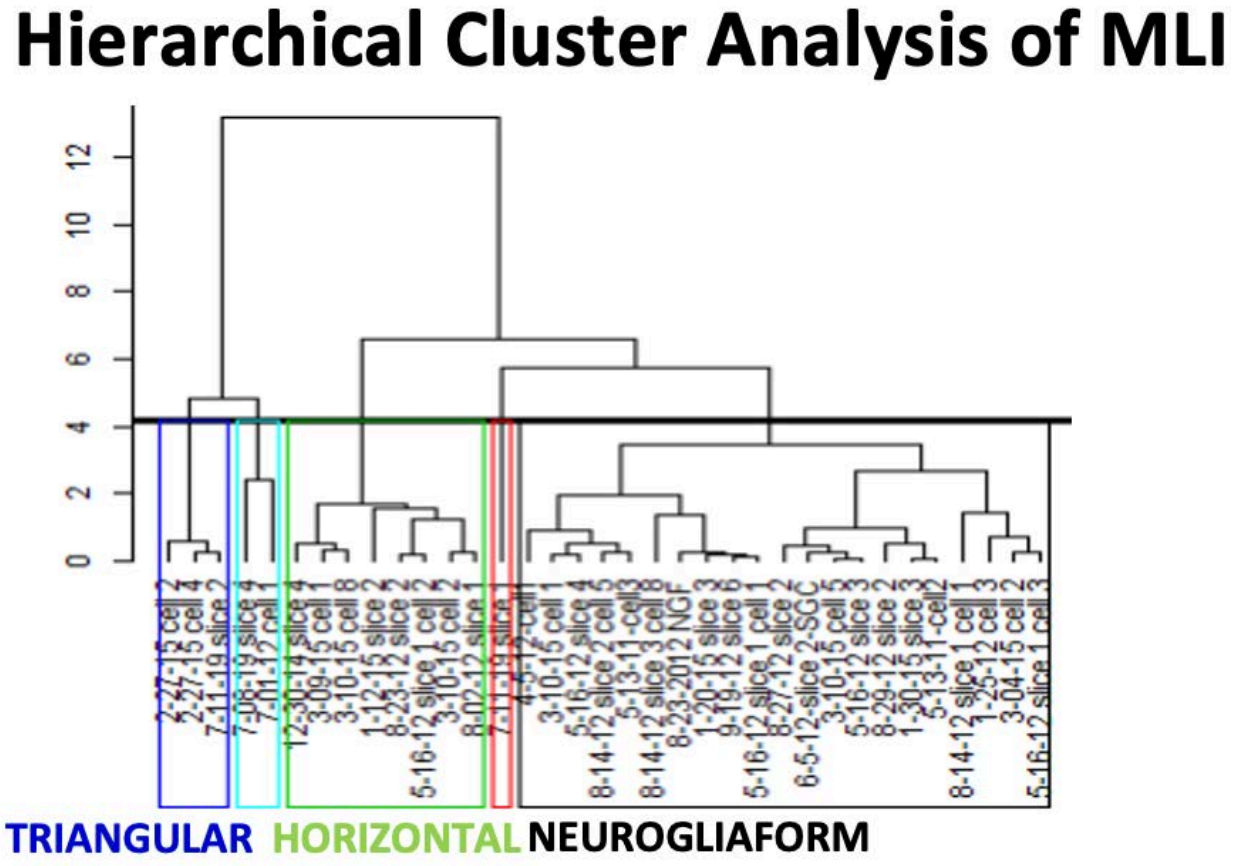

FIGURE 14: Hierarchical Cluster Analysis of MLI with Classifications

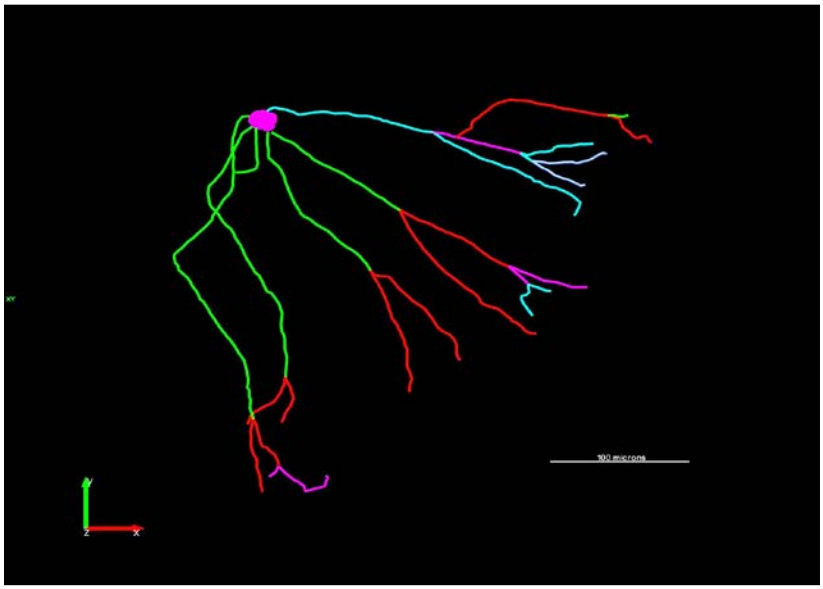

FIGURE 15: Reconstruction of SGC from Red Cluster in Hierarchical Analysis

Overview of Cell Types

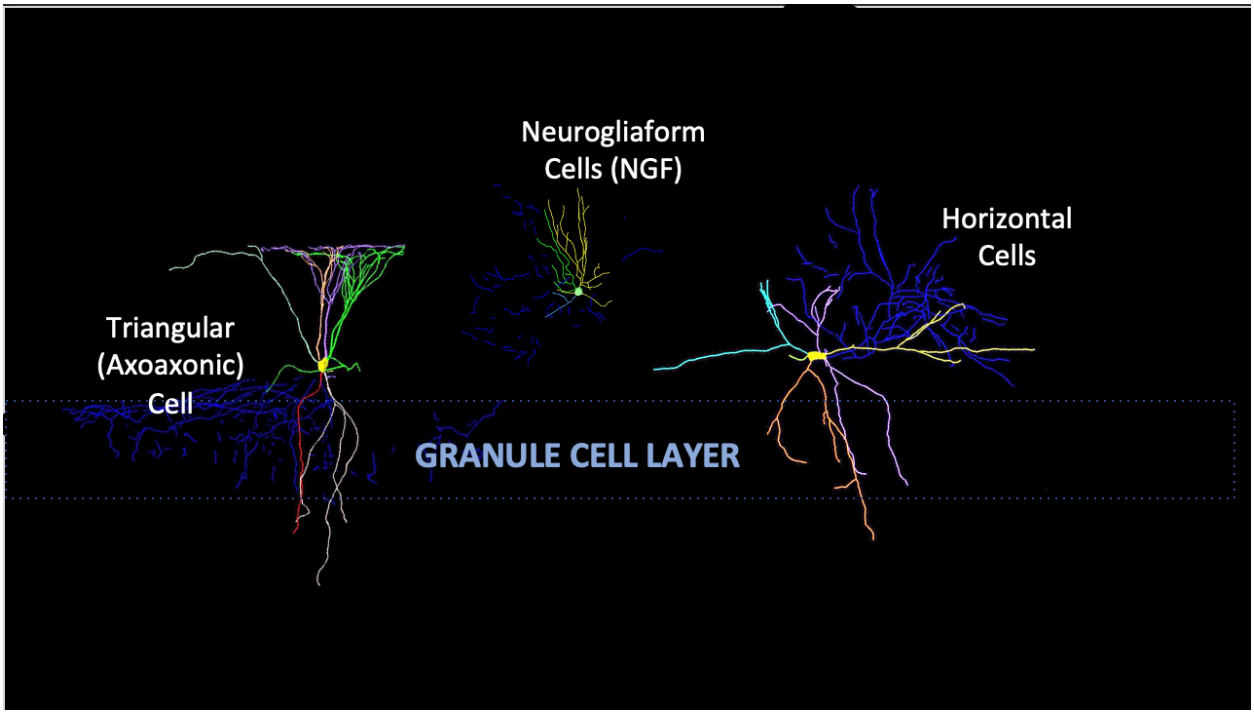

FIGURE 16: Overview of MLI in the Three Layers of the Dentate Gyrus

Shown above is an overview of the three major clusters of molecular layer interneurons and their respective location within the three layers of the dentate gyrus (**FIGURE 16**). We can

see that the triangular cell's dendrites span throughout all the layers of the dentate gyrus and its axons, in blue, tend to stay primarily within the granule cell layer. These are relatively large cells with their soma positioned near the inner boundaries of the molecular layer. This triangular cell, in particular, is a class of axoaxonic cells. It resembles a chandelier due to its axons having a unique distribution pattern as they form vertical axon terminal boutons within the granule cell layer (Wang et al. Review). The Neurogliaform cells are much smaller cells as shown by the 100-micron scale bar images (**FIGURE 6**). The somata of these cells are located in the upper boundaries of the molecular layer, and both their dendrites and axons stay in close proximity within the molecular layer. Due to their position, Neurogliaform cells are shown to have high presynaptic bouton density, as well as an unusually large distance from their postsynaptic targets (Overstreet-Wadiche and McBain, 2015). Lastly, the novel class of horizontal cells are quite large, similar in size to the two clusters of triangular cells. Their uniquely shaped horizontal soma is positioned in the inner boundaries of the molecular layer, and similar to the triangular cells, they also have dendritic processes extend across the three layers of the dentate gyrus. However, when comparing axonal distribution, the axons of the horizontal cells remain within the molecular layer.

Summary of Morphological Parameters

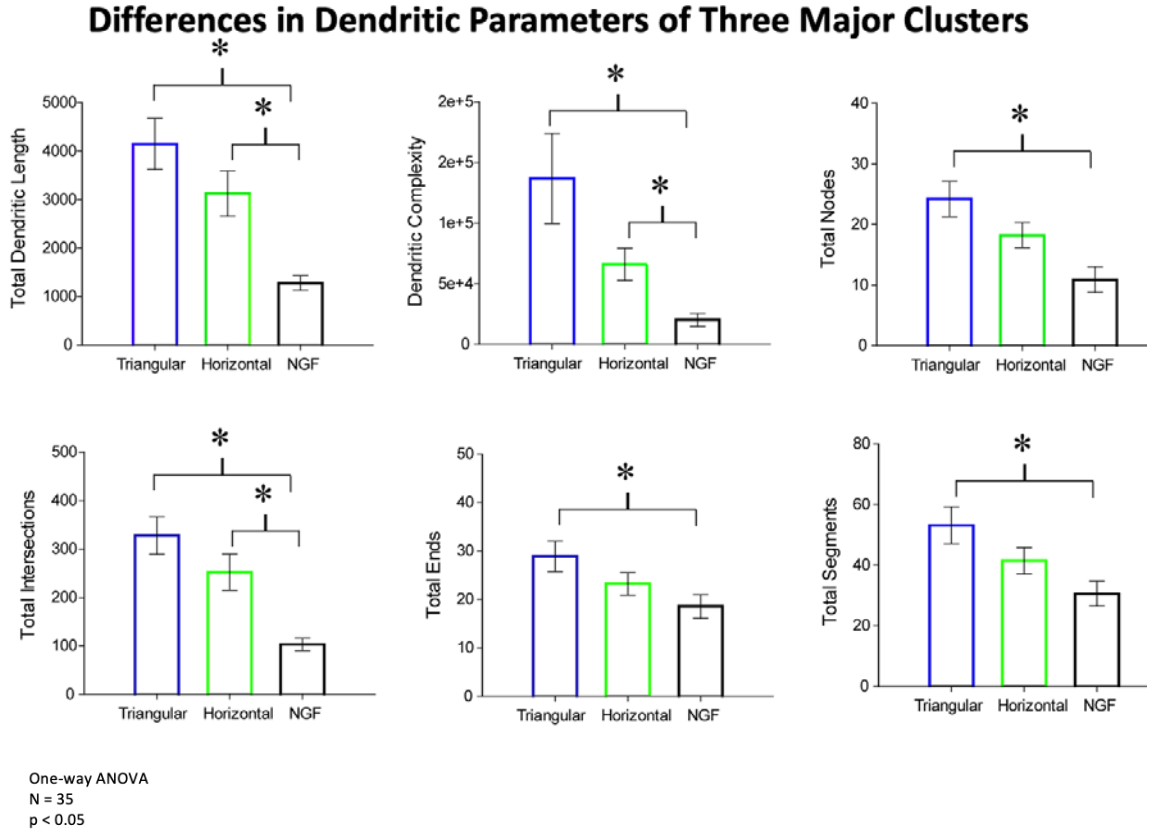

FIGURE 17: Bar Graphs Displaying Differences in Dendritic Parameters of Three Clusters

After analyzing the seventy-one objective parameters, we focused on narrowing down the comparison to global parameters as shown above. Summary plots were generated in order to quantitatively depict the differences between the three major clusters primarily through comparison of somato-dendritic parameters (**FIGURE 17**). We observed a trend in which certain global parameters from triangular cells were significantly greater than cells in the other two clusters. For example, the triangular cells had the longest total dendritic length and the most dendritic complexity when compared to horizontal cells and Neurogliaform cells. Similarly, the Neurogliaform cells had both the shortest total dendritic length and the least dendritic complexity out of the three clusters, as noted earlier in discussion about their size and proximity (**FIGURE 16**).

Discussion

Literature on the interneurons within the molecular layer of the hippocampal dentate gyrus has shown the identification of several cell types such as Neurogliaform Cells and a class of Axoaxonic cells. Neurogliaform cells present as a class of relatively small GABAergic inhibitory interneurons that reside within the upper boundaries of the molecular layer (Overstreet-Wadiche and McBain Review 2015). Axoaxonic cells, similarly, have been characterized as GABAergic interneurons with expansive connectivity to the axon initial segment of pyramidal neurons which is the site of action potential generation (Wang et al. 2016). Using the unbiased hierarchical cluster analysis across seventy-one objective morphological parameters, we were able to generate distinct clusters of interneuronal subtypes. Within this, we identified a novel interneuronal subtype which consisted of cells with a uniquely shaped horizontal somata. The location of these cells pertained to their somata remaining close to the boundary of the molecular layer and granule cell layer with dendritic processes that extended through all three layers of the hippocampal dentate gyrus.

There were several limitations in this study of analyzing the structure of the molecular layer interneurons based on anatomical features. Complete axonal data was not used in generating parameters for analysis, so the focus was limited to somato-dendritic features. Furthermore, physiological parameters were not included in the current analysis, rendering it difficult to assess relationships between the structure and functional features of these cells. Thirty-five cells and their reconstructions were used, but a higher sample number is required for further analysis of these morphological parameters. Our data, however, provides objective comparisons of these anatomical features through quantitative features such as total dendritic length, dendritic complexity, and numerical values for segment length, total nodes, and number

of primary dendrites. Furthermore, the data was generated through unsupervised analysis and a blind statistical study to remove bias from determining the clusters.

Further studies analyzing axonal parameters can provide more in-depth discussion of the morphological classifications of these clusters. With the somato-dendritic parameters presented in this study, physiological data can be researched and included to relate structure and function such as the role of horizontal cells in the inhibitory circuit as their dendritic processes extend throughout all three layers of the dentate gyrus.

Conclusion

In a study of the molecular layer interneurons of the hippocampal dentate gyrus, we used morphological analysis to establish three structurally different cell types: triangular cells, horizontal soma cells, and Neurogliaform cells. Structure forms the foundation for integrating input of information through the dendrites, determines output of information through the axons, and can provide insights into the role played by distinct types of molecular layer interneurons within the circuit. How the differences in structural properties lead to physiological differences with each cell type having a role that needs to be further studied.

References

Gupta, A., Subramanian, D., Proddutur, A., Chang, Y., Guevarra, J., Shah, Y., Elgammal, F., & Santhakumar, V. (2019). Semilunar Granule Cells Maintain Distinct Dendritic Morphology and Inhibition through Postnatal Development and Receive Heightened Inhibition in Adolescence. doi: 10.3791/54880

Gupta, A., Subramanian, D., Proddutur, A., Chang, Y., Raturi, V., Guevarra, J., Shah, Y., Elgammal, F., & Santhakumar, V. (2019). Dendritic Morphology and Inhibitory Regulation Distinguish Dentate Semilunar Granule Cells from Granule Cells through Distinct Stages of Postnatal Development. doi: 10.1101/2019.12.17.880005

Swietek, B., Gupta, A., Proddutur, A., & Santhakumar, V. (2016). Immunostaining of Biocytin-filled and Processed Sections for Neurochemical Markers. *Journal of visualized experiments: JoVE*, (118), 54880. https://doi.org/10.3791/54880

Freund, T.F., Buzsaki, G. ((1996). Interneurons of the hippocampus. *Hippocampus*. 6:347-470. doi: 10.1002/(SICI)1098-1063(1996)6:4<347::AID-HIPO1>3.0.CO;2-I

Anand, K. S., & Dhikav, V. (2012). Hippocampus in health and disease: An overview. *Annals of Indian Academy of Neurology*, *15*(4), 239–246. https://doi.org/10.4103/0972-2327.104323

Klausberger T., Somogyi P. (2008). Neuronal diversity and temporal dynamics: the unity of hippocampal circuit operations. *Science*. 2008;321(5885):53-57. doi:10.1126/science.1149381

Wang, Y., Zhang, P., & Wyskiel, D. (2016). Chandelier Cells in Functional and Dysfunctional Neural Circuits. https://doi.org/10.3389/fncir.2016.00033

Overstreet-Wadiche, L., McBain, C. Neurogliaform cells in cortical circuits. *Nature Review Neuroscience* 16, 458–468 (2015). https://doi.org/10.1038/nrn3969

Appendix

TABLE 1: Definitions of Somatic Parameters

SOMATIC PARAMETERS			
Parameter	**Acronym**	**Equations**	**Definitions: MBF BIOSCIENCE** https://www.mbfbioscience.com/help/neurolucida_explorer/Content/Analyze/Branched%20Structure/neuronSumm.htm?Highlight=cell%20body%20details
Soma Volume	Svol		Calculations for the cell body were accomplished by dividing the soma into stacks with equal thickness and quantifying the summed volume of the stacks.
Surface Aea of soma	Sarea	*[(perimeter Contour 1 + perimeter Contour 2 + ... + perimeter Contour n)/n] * thickness*	Addition of outer surface area of stack of all the contours.
Soma Width	Swith		Measure of the largest distance in soma parallel to the hilar border
Somatic parameters related to largest soma cross section based on highest perimeter			
Contour	Cont		Each slice division of the soma
Feret Max	Feret.X		The largest dimensions of the contour as if a caliper was used to measure across the contour.
Aspect ratio	S_Asp_Rt		This is a 2D parameter of soma contour defined as the ratio of its minimum diameter to its maximum diameter. [Range of values is 0-1. A circle has an aspect ratio of 1]
Compactness	S_Cmpct	$\sqrt{\frac{4}{\pi} * AREA}$/ Max Diameter	2D parameter describes the relationship between the area and the maximum diameter. [Range of values is 0 to 1. A circle is the most compact shape with compactness = 1].
Form factor	S_Form	$4\pi * AREA$/ (perimeter)^2	The form factor differs from the compactness by considering the complexity of the perimeter of the object. As the contour shape approaches that of a perfect circle, this value approaches a maximum of 1.0.
Roundness	S_Rnd	[Compactness]^2	Roundness is the square of the compactness to enable discrimination of objects with small compactness values.
Convexity	S_xity	Convex perimeter/Perimeter	A completely convex object does not have indentations, and has a convexity value of 1 (e.g., circles, ellipses, and squares). Concave objects have convexity values less than 1.
Solidity	S_solid	Area/Convex area	Solidity is the area of the contour divided by the convex area. The area enclosed by a 'rubber band' stretched around a contour is called the convex area. • Circles, squares, and ellipses have a solidity of 1. • Indentations in the contour take area away from the convex area, decreasing the actual area within the contour. Note that it is possible to have contours with low convexity and high solidity, and vice versa.
Perimeter	Speri	*Perimeter +/- (Perimeter Error Coefficient * Max distance from contour boundary in microns)*	Refers to the length of the contour for either open or closed contours. The length takes the Z positions of the coordinates into account.

TABLE 2: Definitions of Dendritic Parameters

Parameter	Acronym	Equations	Definitions: MBF BIOSCIENCE- https://www.mbfbioscience.com/help/neurolucida_explorer/Content/Analyze/Branched%20Structure/neuronSumm.htm?Highlight=cell%20body%20details
Centrifugal Ordering and Branch orders			The centrifugal ordering scheme is used to assign branch order to a tree. The segment that begins at the origin of the dendrite is assigned the branch order **1**. The branches that connect to that segment are assigned the branch order **2** and so on until all branches are assigned a value.
Tortuosity	Tort	Tortuosity = [Distance along process] / [Straight line distance]	The smallest tortuosity possible is 1—This is a straight path. Tortuosity increases as the segment assumes a more complex path to reach its destination. Tortuosity allows segments of different lengths to be compared in terms of the complexity of the paths they take.
Primary	prim		Number of dendrites originating directly from soma.
Primary Secondary, tertiary, quaternary Dendritic segments	x1segm, x2segm, x3segm & x4segm		Number of dendritic segments in first, second, third and fourth order dendrites respectively. Note X1SEGM is the same as PRIM
Primary, Secondary tertiary, length	x1lth, x2lth, x3lth & x4lth		Summed lengths of all segments in a given dendritic order
Totals terminals, Primary Secondary, tertiary, quaternary Terminals	end, x1end, x2end, x3end & x4end		Number of distal ends or terminals of dendritic segments that don't divide further
Dendritic Length	D_Lth	x1lth + x2lth + x3lth…….	Total length of all the dendrites
Dendritic Mean Length	D_MnLth	D_Lth / no. of primary dendrites	Length per dendritic tree arising from soma
Angle	ang		Two dimensional measurement of angle subtended by the most distal of the most distant dendrites at the center of soma
Space volume of cell	D_Area	Convex Hull	Volume of the space occupied by the dendritic arbors of the cell
Surface Area of space occupied by cell	D_Volume	Convex Hull	Surface area of the space occupied by the dendritic arbors of the cell
Dendritic Complexity	D_Cmplx	[Sum of the terminal orders + Number of terminals] * [Total dendritic length / Number of primary dendrites]	A parameter that normalizes and compares distribution of dendrites among fundamentally different neurons
Maximum Order	MxOrdr		Maximum order up to which dendritic segments reach.